Chinese Chemical Letters 37 (2026) 110859

Contents lists available at ScienceDirect

Chinese Chemical Letters

journal homepage: www.elsevier.com/locate/cclet

Alkaline lysine additive enables highly stable Zn anode for aqueous zinc-ion batteries

Guangbin Wang[a,1], Binrui Xu[b,1,*], Bo Zhao[a,c,1], Yifei Pei[a], Haoming Li[a], Wanhong Zhang[a,*], Yong Liu[a,*]

[a] School of Material Science and Engineering, Provincial and Ministerial Co-Construction of Collaborative Innovation Center for Non-Ferrous Metal New Materials and Advanced Processing Technology, Henan University of Science and Technology, Luoyang 471023, China
[b] School of Information Engineering, Henan University of Science and Technology, Luoyang 471023, China
[c] Key Laboratory of Cluster Science of Ministry of Education, Beijing Key Laboratory of Photoelectronic/Electrophotonic Conversion Materials, School of Chemistry and Chemical Engineering, Beijing Institute of Technology, Beijing 100081, China

ARTICLE INFO

Article history:
Received 25 December 2024
Revised 6 January 2025
Accepted 14 January 2025
Available online 15 January 2025

Keywords:
Zn anode
Electrolyte additive
Zinc dendrite
Side reactions
Electrochemical performance

ABSTRACT

Rechargeable aqueous zinc-ion batteries (RAZIBs) have been considered as viable alternatives to lithium-ion batteries in electrochemical energy storage due to their intrinsic safety, low cost, and environmental friendliness. However, the further practical application of RAZIBs is restricted by the growth of zinc dendrites and severe side reactions during cycling. To address these issues, we proposed a new lysine (Lys) additive to the $ZnSO_4$ electrolyte, the hydrolyzed Lys^+ cations can be adsorbed on the Zn anode's surface to modify the interface between the zinc electrode and the $ZnSO_4$ electrolyte. This modification helps weaken the "tip effect" and guides the uniform zinc deposition, effectively alleviating the formation of zinc dendrites. Additionally, introducing alkaline Lys can regulate the pH value of the $ZnSO_4$ electrolyte and suppress side reactions, thereby decreasing the production of by-products. Consequently, the Zn||Zn symmetric cell with Lys additive stably cycled for 4500 h at 1 mA/cm^2, and the Zn||$NH_4V_4O_{10}$ full cell with Lys additive exhibited improved performance (with a capacity retention of 72 % after 1000 cycles) at 5 A/g. This strategy provides valuable insights for developing stable Zn anode toward high-performance RAZIBs.

© 2026 Published by Elsevier B.V. on behalf of Chinese Chemical Society and Institute of Materia Medica, Chinese Academy of Medical Sciences.

With the excessive exploration and consumption of fossil fuels, environmental pollution and energy crisis become increasingly severe [1]. To solve these two issues, the exploration and usage of renewable green energy have become increasingly important and have gotten broad attention worldwide [2]. Although the development of renewable green energy has been made great progress in the last few decades, these renewable energies such as solar energy and wind energy still suffer from their inherent intermittence and fluctuation, greatly hindering their further developments [3,4]. In this regard, electrochemical energy storage (EES) devices are considered as one of the most promising solutions to solve these problems mentioned above of renewable energies [5–10]. Among different types of EES devices, RAZIBs have attracted widespread attention because of their abundance of resources, environmental friendliness, intrinsic safety, high specific capacity (820 mAh/g), and moderate redox potential (−0.76 V *vs.* standard hydrogen electrodes) [11,12]. Nevertheless, several severe issues need to be addressed before the large-scale application of RAZIBs, including the notorious growth of zinc dendrites [13–21], side-reactions (hydrogen evolution reactions (HER), corrosion, *etc.*) [22–24], resulting in unsatisfactory Coulombic efficiency (CE) and inferior cycling stability [25–29].

To tackle these challenges, various approaches have been explored, including constructing artificial SEI on the Zn anode [30–34], modification of the separator [35–37], and electrolyte engineering [2,38–41]. Among these methods, electrolyte engineering is considered to be one of the most simple and effective strategies to enhance the electrochemical performance of RAZIBs [2]. To date, numerous additives have been proposed to enhance the stability of the zinc anode. For example, Zhang and co-workers introduced hydrophilic graphene quantum dots to the $ZnSO_4$ electrolyte [42], in which the oxygen-containing groups of graphene quantum dots could bind with Zn^{2+} and induce uniform Zn deposition. The Zn||Zn symmetric cell with the addition of graphene quantum dots exhibited a long cycling lifespan (2200 h at 0.8 mA/cm^2). Further-

* Corresponding authors.
E-mail addresses: 9906065@haust.edu.cn (B. Xu), zhangwh@haust.edu.cn (W. Zhang), liuyong209@haust.edu.cn (Y. Liu).
[1] These authors contributed equally to this work.

https://doi.org/10.1016/j.cclet.2025.110859
1001-8417/© 2026 Published by Elsevier B.V. on behalf of Chinese Chemical Society and Institute of Materia Medica, Chinese Academy of Medical Sciences.

more, Wang *et al*. used graphene oxide as a novel electrolyte additive with good dispersion in aqueous $ZnSO_4$ electrolyte, which significantly boosted the stability of zinc anode by realizing the uniform deposition morphology of Zn [43]. Although the above-mentioned additives significantly improve the electrochemical performance of the RAZIBs, their expensive price is not conducive to the large-scale promotion of the RAZIBs. Therefore, it is urgent to develop a cost-effective electrolyte additive to further facilitate the practical application of RAZIBs. Recently, aminol acid additives, such as glycine [44], arginine [45,46], histidine [47,48], and threonine [49] have attracted a considerable amount of attention in the field of RAZIBs because of their rich functional groups, high safety, low cost, and environmental friendliness. For instance, Yang *et al*. added 3 mol/L glycine to a 1 mol/L $ZnSO_4$ electrolyte, which could stabilize the Zn anode by suppressing HER and inhibiting the growth of zinc dendrites [44]. Nevertheless, the high concentration of the glycine additive largely increased the cost of electrolyte and hindered its large-scale application. To the best of our knowledge, lysine (Lys) additive has been rarely reported for RAZIBs, and especially its working mechanism on stabilizing Zn anode has not been systematically investigated.

Herein, a newly low-cost and effective Lys additive was introduced into an aqueous $ZnSO_4$ electrolyte to improve the electrochemical performance of the zinc anode. Lys is an alkaline amino acid with good solubility in aqueous $ZnSO_4$ electrolytes and can form Lys^+ cations by alkaline hydrolysis [50]. Thereby, Lys can increase the pH value of the $ZnSO_4$ electrolyte, significantly suppressing the corrosion reaction of the zinc metal as well as inhibiting the HER. Moreover, theoretical calculation and experimental results demonstrated that the Lys^+ could adsorb on the zinc anode's surface which can provide an electrostatic shielding layer and regulate the electrolyte-electrode interface, greatly suppressing the dendrites' growth in the Zn plating process. As a result, both the Zn||Zn symmetric cell and Zn||$NH_4V_4O_{10}$ full cell with Lys additive exhibited enhanced cycling stability and improved electrochemical performances.

Lys, a basic amino acid, is known for its safety, environmental friendliness, and cost-effectiveness [51,52]. To assess the effect of the Lys additive on regulating the deposition and stripping behavior of the Zn anode, the galvanostatic charging-discharging test was conducted on Zn||Zn symmetric cells in 3 mol/L $ZnSO_4$ electrolytes with and without the Lys additive. Fig. 1a shows that a short circuit occurred in the Zn||Zn cell with the bare $ZnSO_4$ electrolyte after only 100 h at 1 mA/cm^2, possibly due to the zinc dendrites formation on the Zn anode's surface. The symmetric cells using electrolytes with varying concentrations of Lys (10 mmol/L and 150 mmol/L) failed after cycling for 120 h and 2000 h, respectively (Figs. S2a and b in Supporting information), while the cells using electrolytes with 50 mmol/L and 100 mmol/L Lys (Fig. S2c in Supporting information) exhibited outstanding cycling performance (4500 h). Moreover, the cell using the electrolyte with 50 mmol/L Lys demonstrated a more stable cycling with lower polarization voltage (Fig. 1b) compared to 100 mmol/L Lys (Fig. S2d in Supporting information) at 5 mA/cm^2, which may be because high concentrate Lys hindered the charge transfer of Zn^{2+} and was not favorable for the long-term cycling of the Zn anodes [49]. Hence, 50 mmol/L was chosen as the optimal concentration of the Lys additive in the 3 mol/L $ZnSO_4$ electrolyte (named $ZnSO_4$+Lys). In addition, the rate performance depicted in Fig. S3 shows that the Zn||Zn symmetric cell with $ZnSO_4$+Lys electrolyte maintains stable cycling across varying current densities, whereas the cell with the bare $ZnSO_4$ electrolyte fails rapidly, indicating that the Lys additive can strengthen the stability of the Zn anodes. Furthermore, the Lys additive demonstrated a superior ability to boost the stability of the Zn anode compared to other electrolyte additives in previous research (Fig. 1c and Table S1 in Supporting information), which is among the longest cycling life under similar testing conditions. The long-term cycling test (Fig. 1a and Fig. S2 in Supporting information) indicated that the polarization voltage of the Zn||Zn cells increased along with the concentration of the Lys additive, indicating that Lys affected the Zn plating/stripping kinetics.

A further investigation into the kinetics was carried out by measuring the electrochemical impedance spectroscopy (EIS) of the Zn||Zn symmetric cells using different electrolytes, as depicted in Fig. S4 (Supporting information). It can be observed that the $ZnSO_4$+Lys electrolyte delivered higher charge transfer resistance than the bare $ZnSO_4$ electrolyte even after the activation of the electrode-electrolyte interface, leading to a higher polarization voltage. This can be ascribed to the steric hindrance of the charged Lys adsorption layer [53]. It is worth noting that the charge transfer resistance of the symmetric cells decreased during cycling, indicating the enhanced Zn deposition/stripping kinetics, which is mainly because the cycling process activated the electrode-electrolyte interface [54]. And the adsorption behavior of the Lys additive will be clarified in the part of the mechanism analysis. The ion conductivity of the bare $ZnSO_4$ and $ZnSO_4$+Lys electrolytes as well as their viscosity were also measured (Figs. S5 and S6 in Supporting information). The findings revealed that the ion conductivity slightly increased with a decrease in viscosity, which might be ascribed to the increased amount of the charge carrier (Lys^+) and the addition of the dilute H_2SO_4 solution (pH value: 1.4) [55]. Moreover, as shown in Fig. S7 (Supporting information), the $ZnSO_4$+Lys electrolyte shows higher contact angle (97.8°) than the bare $ZnSO_4$ electrolyte (92.7°), indicating that the wettability of the $ZnSO_4$ electrolyte was decreased after the introduction of the Lys additive [56], and this is a reason for the increased charge transfer resistance of the symmetric cells when using the $ZnSO_4$+Lys electrolyte. As a result, the introduction of Lys additive into the bare $ZnSO_4$ electrolyte did not accelerate the charge transfer in the cells but strengthened the stability of the Zn anode.

To understand the diffusion behavior of zinc ions, *I-t* (current-time) test was conducted on the Zn||Zn symmetric cells. In the test lasting 150 s, the current in the bare $ZnSO_4$ electrolyte showed a continuous increase, as depicted in Fig. 1d. This behavior suggested that the random diffusion of Zn^{2+} was predominantly governed by 2D diffusion, which predisposed the system to uneven deposition and severe dendrite growth [57]. In contrast, a transition from 2D to 3D diffusion behavior (evidenced by the stable current density) occurred within 25 s when using the $ZnSO_4$+Lys electrolyte, implying a trend towards uniform Zn deposition. Additionally, the deposition morphology of the Zn anode at 50th cycle was scrutinized *via* scanning electron microscopy (SEM) (Figs. 1e–g). After cycling in the bare $ZnSO_4$ electrolyte, the surface of the Zn anode exhibited unevenness and was covered with random flakes. However, the Zn anode cycled in the $ZnSO_4$+Lys electrolyte exhibited a smooth morphology without flakes. These results highlighted the inhibitory effect of the Lys additive on the random diffusion of Zn ions, facilitating uniform Zn deposition and thereby mitigating the dendrites growth.

To evaluate the reversibility of the Zn anode in the charging-discharging process, the CE was measured by using Zn||Cu half cells (Fig. 2a) [58]. The Zn||Cu half cell with the bare $ZnSO_4$ electrolyte showed instability after only 60 cycles, and the CE dropped below 50 %. On the contrary, the cell utilizing the $ZnSO_4$+Lys electrolyte maintained a stable and high CE over 99 % for 1200 cycles, unveiling the outstanding reversibility of Zn plating/stripping. The corresponding capacity–voltage curves are shown in Fig. 2b. The Zn||Cu half cell using the bare $ZnSO_4$ electrolyte failed to charge to 0.6 V in the 60th cycle, in contrast, the cell with the $ZnSO_4$+Lys electrolyte exhibited consistent charging and discharging throughout the test process. The Zn nucleation process is vital for the reversibility of the Zn anode. Hence, the nucleation overpotential

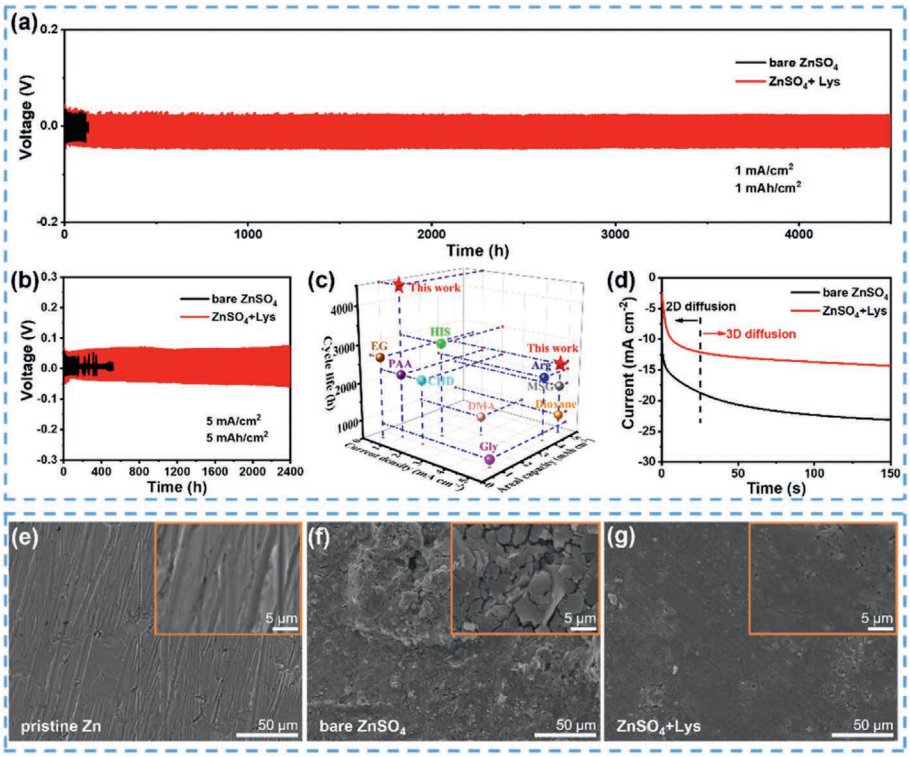


Fig. 1. Stability of the Zn anode in different electrolytes at (a) 1 mA/cm^2 and 1 mAh/cm^2, and (b) 5 mA/cm^2 and 5 mAh/cm^2. (c) Comparison of the cycling lifespan of the symmetric cells with different electrolyte additives. (d) *I-t* curves of Zn||Zn symmetric cells in the bare $ZnSO_4$ electrolyte and the $ZnSO_4$+Lys electrolyte. Surface morphology of the Zn electrodes: (e) before cycling, (f) after 50 cycles in the bare $ZnSO_4$ electrolyte, and (g) after 50 cycles in the $ZnSO_4$+Lys electrolyte.

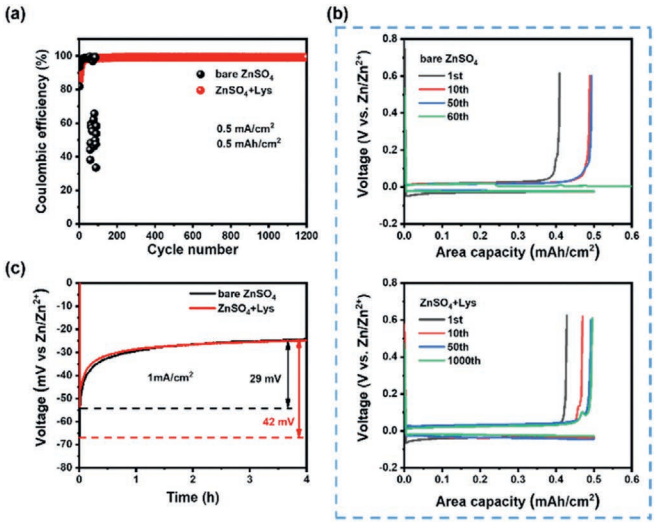


Fig. 2. (a) Performance of Zn plating–stripping on Cu electrode in the pure $ZnSO_4$ electrolyte and in the $ZnSO_4$+Lys electrolyte and (b) the corresponding capacity–voltage curves in different cycles. (c) NOP in the pure $ZnSO_4$ electrolyte and the $ZnSO_4$+Lys electrolyte.

(NOP) was tested at 1 mA/cm^2, as shown in Fig. S8 (Supporting information) and Fig. 2c. It was observed that the introduction of Lys additive increased the NOP of the Zn on the Cu electrode, leading to finer nucleation and uniform deposition of Zn, which is consistent with the morphology images of Zn anodes (Fig. 1g) [46].

Zn anodes were soaked separately in the bare $ZnSO_4$ electrolyte and the $ZnSO_4$+Lys electrolyte for 10 days to study the influence of the Lys additive on suppressing side reactions. SEM images of the Zn anodes after soaking are shown in Figs. 3a and b. The Zn anode soaked in the bare $ZnSO_4$ electrolyte exposed an uneven surface with obviously blocky by-products, suggesting the occurrence of side reactions. By contrast, the smooth surface of the Zn anode cycled in the $ZnSO_4$+Lys electrolyte indicated that the Lys additive effectively suppressed dendrites and side reactions. Furthermore, the Nyquist curve revealed that the Zn||Zn symmetric cell in the bare $ZnSO_4$ electrolyte exhibited a smaller charge transfer impedance than the cell in the $ZnSO_4$+Lys electrolyte (Figs. 3e and f). However, both cells showed an increase in the charge transfer impedance after settling for 24 h. Notably, the addition of Lys in the $ZnSO_4$+Lys electrolyte resulted in a smaller charge transfer impedance compared to the pristine $ZnSO_4$ electrolyte. This observation indicates that the Lys additive has the potential to impede the generation of undesired by-products resulting from side reactions [59,60], which can impede ion diffusion and charge transfer. To further investigate the mechanism of the Lys additive on the side reactions inhibition, Tafel and LSV tests were performed. The corrosion current (1.223 mA/cm^2) of the cell with the $ZnSO_4$+Lys electrolyte was significantly lower than that with the bare $ZnSO_4$ electrolyte (2.765 mA/cm^2), as shown in Fig. 3c. In addition, Fig. 3d shows that the HER potential (−119 mV) in the $ZnSO_4$+Lys electrolyte is 32 mV lower than that (−87 mV) in the bare $ZnSO_4$ electrolyte, implying that the introduction of Lys can suppress the HER in RAZIBs [61]. Moreover, *in-situ* optical microscopy observations during the Zn deposition process showed numerous bubbles in the bare $ZnSO_4$ electrolyte (Fig. 3g), whereas no bubbles were observed when using the $ZnSO_4$+Lys electrolyte (Fig. 3h). This observation further confirmed the excellent HER-suppressing ability of the Lys additive.

To further analyze the structure change of the water molecules in the electrolyte after Lys additive modification, the $ZnSO_4$ electrolytes with and without Lys were characterized by Fourier transform infrared (FTIR) spectra. After introducing the Lys additive in the $ZnSO_4$ electrolyte, a blue shift in the H–O bending vibration

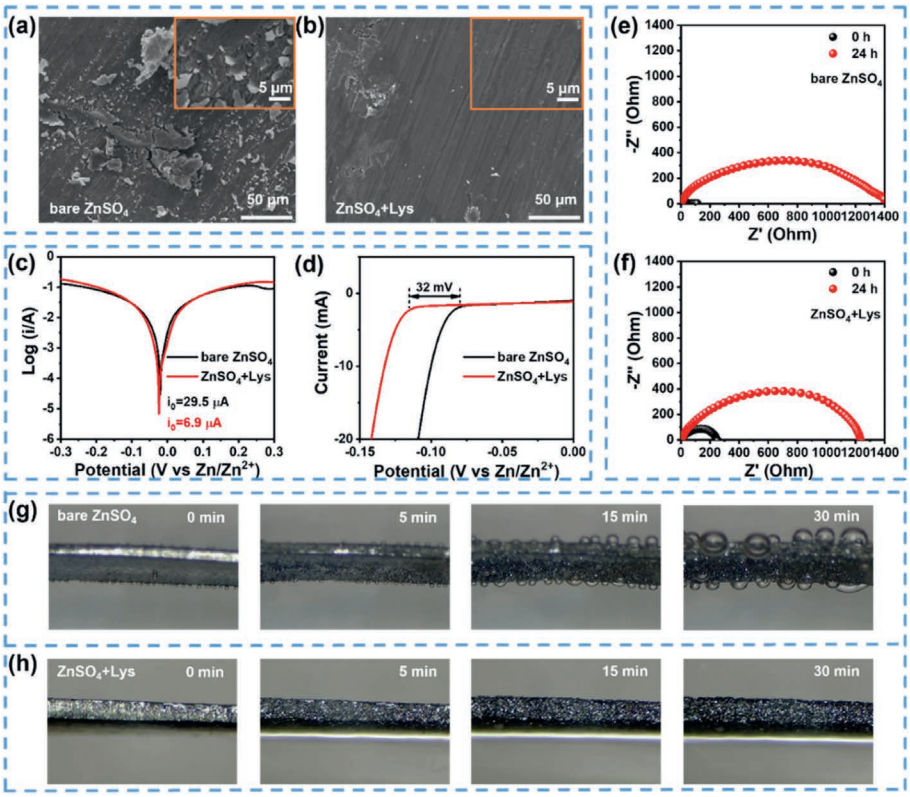


Fig. 3. Surface morphology of the Zn electrode after soaking for 10 days in (a) the bare $ZnSO_4$ electrolyte and (b) the $ZnSO_4$+Lys electrolyte. (c) Tafel plots of Zn||Zn symmetric cell in the bare $ZnSO_4$ electrolyte and the $ZnSO_4$+Lys electrolyte. (d) LSV curve of the bare $ZnSO_4$ electrolyte and the $ZnSO_4$+Lys electrolyte. EIS of symmetric cells before and after 24 h with (e) the bare $ZnSO_4$ electrolyte and (f) the $ZnSO_4$+Lys electrolyte. *In-situ* microscopy image of the Zn electrode during the process of Zn deposition in (g) the bare $ZnSO_4$ electrolyte and (h) the $ZnSO_4$+Lys electrolyte.

observed in the FTIR spectra (Fig. 4a) from 1641 cm^{-1} to 1645 cm^{-1} was observed, along with a shift in the H–O stretching vibration to a higher frequency (Fig. S9 in Supporting information). The FTIR results indicated a decrease in the water molecules' activity and the suppression of HER [62]. Additionally, the zeta potential (Fig. 4b) showed an increase from −2.09 mV to 2.36 mV when the $ZnSO_4$ electrolyte was optimized by Lys, this might be attributed to the presence of Lys^+ cations [63]. Moreover, X-ray photoelectron spectroscopy (XPS) measurement was performed to clarify whether the Lys additive is bound to the zinc anode's surface. As illustrated in Fig. S10 (Supporting information), the XPS spectra revealed minimal N content on the Zn anode's surface in both electrolytes with and without Lys. Furthermore, there was no discernible difference in the binding energy of Zn 2p (Fig. 4c). This might be ascribed to the dynamic adsorption of the Lys^+ cations on the zinc anode, rather than binding or molecule adsorption.

To evaluate the adsorption capability behavior of the Lys additive on the zinc anode, the adsorption energy (Fig. 4d) of H_2O, Lys, and Lys^+ on the zinc anode's surface was calculated by density functional theory (DFT) calculation. It was found that the adsorption energy of Lys (−1.27 eV) surpasses that of H_2O molecules (−0.28 eV) on the Zn anode, and Lys^+ exhibits the highest adsorption energy of −6.24 eV, highlighting its propensity for surface adsorption [45]. To further verify the self-adaptability of Lys adsorption, the cyclic voltammetry (CV) curve of the Zn||Zn symmetric cell in $ZnSO_4$+Lys electrolyte is shown in Fig. S11 (Supporting information). A typical capacitive absorption behavior is clarified with no redox peak observed, indicating that the zinc anode-electrolyte interface is dynamic during the Zn plating/stripping process [53]. After the modification of the electrolyte-electrode interface, the absorbed Lys^+ cations can form an electrostatic shielding layer to mitigate the "tip effect". Therefore, Lys effectively suppresses the dendrites formation and side reactions, thereby enhancing the stability and reversibility of the Zn anode.

The regulation effect of the Lys additive is illustrated in Fig. 4e. Zn^{2+} tends to deposit preferentially on the protruding regions of the Zn anode's surface due to the "tip effect", leading to inhomogeneous deposition and the Zn dendrites growth during cycling [64]. Upon the addition of Lys to the bare $ZnSO_4$ electrolyte, Lys is hydrolyzed to form Lys^+, thus increasing the pH value of the electrolyte and suppressing the HER. Moreover, the electrostatic shielding layer (Lys^+ adsorption layer) can alleviate the uneven zinc deposition and suppress the zinc dendrites formation. Therefore, when cycling in the $ZnSO_4$+Lys electrolyte, the zinc deposition is uniform without zinc dendrites and HER.

To evaluate the performance of full cells with the $ZnSO_4$+Lys electrolyte for practical applications, $NH_4V_4O_{10}$ cathodes (Fig. S12 in Supporting information) were used to assemble the full cells. In the CV test (Fig. 5a), the redox peaks correspond to the multi-step V^{5+}/V^{4+} and V^{4+}/V^{3+} redox reaction due to the Zn^{2+} insertion/extraction [55,65]. In detail, during the discharging process of the Zn||$NH_4V_4O_{10}$ full cells with Lys additive, the first small cathodic peak at about 1.32 V is assigned to the occupancy in the intralayer spacing of VO polyhedral [66]. Subsequently, the cathodic peaks at approximately 0.98 V and 0.64 V correspond to the reduction process of V^{5+}/V^{4+} and V^{4+}/V^{3+}, respectively. The corresponding anodic peaks represent the reversible oxidation process. It was observed that the Zn||$NH_4V_4O_{10}$ full cells using $ZnSO_4$ electrolytes with and without Lys showed no significant difference, indicating that the Lys additive had a negligible effect on the electrochemical redox reaction of the Zn|$ZnSO_4$+Lys|$NH_4V_4O_{10}$ full cell without other side reactions [67]. As shown in Fig. 5b, the rate capa-

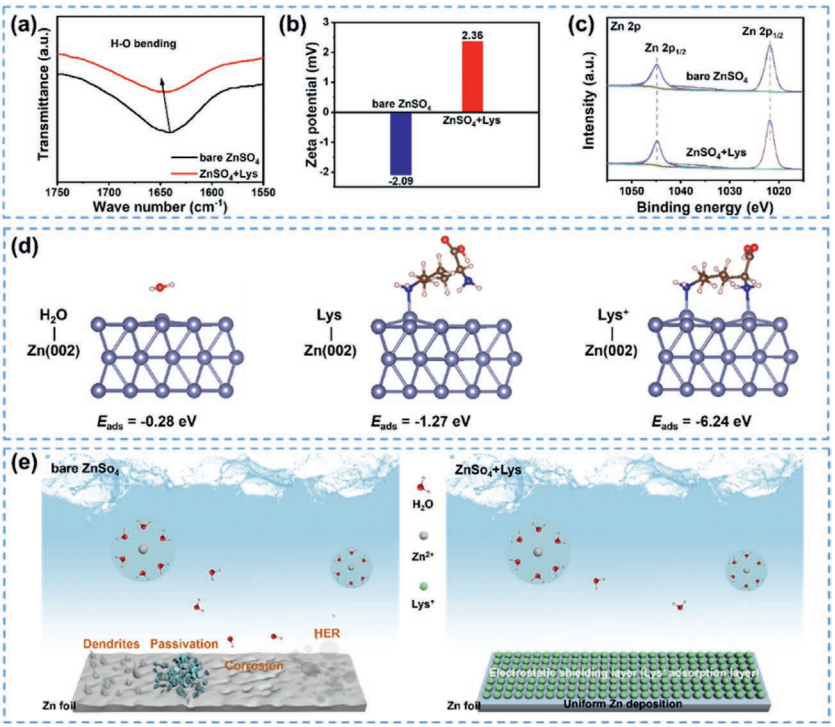


Fig. 4. (a) Fourier transform infrared spectroscopy of the two kinds of electrolyte. (b) Zeta potential of the bare $ZnSO_4$ and $ZnSO_4$+Lys electrolytes. (c) Zn 2p XPS spectroscopy of the Zn electrode after cycling in the bare $ZnSO_4$ electrolyte and the optimized electrolyte. (d) The adsorption energy of H_2O and the uncharged and positively charged Lys on the Zn anode's surface. (e) Illustration of the Zn deposition process in different electrolytes.

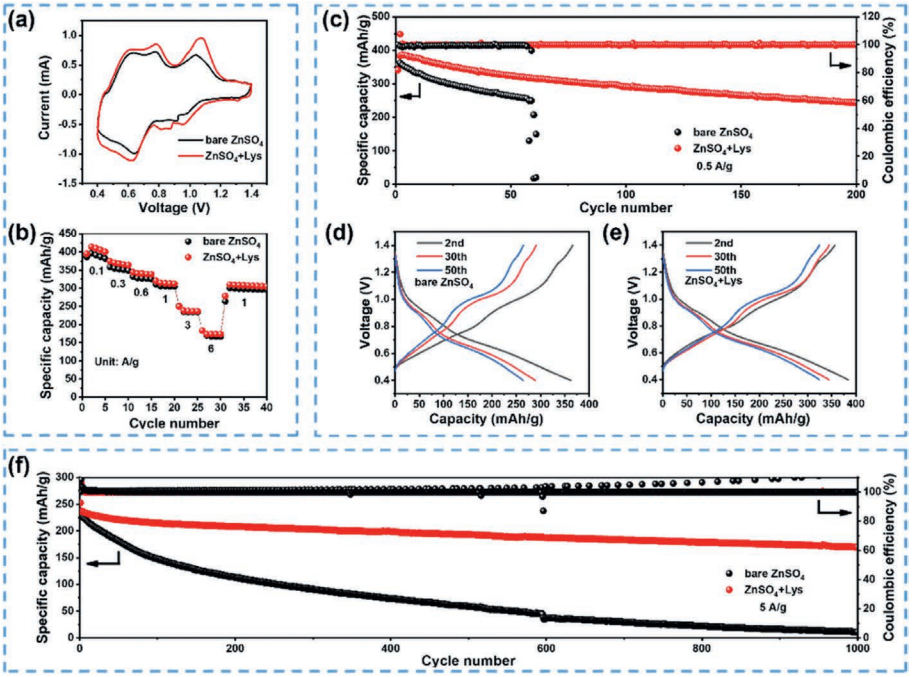


Fig. 5. Electrochemical performance of full cell with an $NH_4V_4O_{10}$ cathode in $ZnSO_4$ without and with Lys. (a) CV curve at a scanning rate of 0.2 mV/s. (b) Rate capability at different current densities. (c) Galvanostatic cycling performance at 0.5 A/g and the corresponding charging–discharging curves for the (d) bare $ZnSO_4$ electrolyte and (e) the $ZnSO_4$+Lys electrolyte. (f) Galvanostatic cycling test at 5 A/g.

bility of the Zn||$NH_4V_4O_{10}$ full cell was also improved. The long cycling performance at 0.5 A/g was then evaluated (Fig. 5c), showing that the Zn|$ZnSO_4$+Lys|$NH_4V_4O_{10}$ full cell exhibited a higher reversible capacity (387 mAh/g) than the Zn|$ZnSO_4$|$NH_4V_4O_{10}$ full cell (362 mAh/g), in line with the larger CV area of the former. Moreover, the cell using the $ZnSO_4$+Lys electrolyte cycled stably for 200 cycles with a high CE of over 99%, whereas the cell with the bare $ZnSO_4$ electrolyte only cycled for 60 cycles with a sharp drop in specific discharge capacity and low CE of 35%. In detail, the charging-discharging curves (Fig. 5d) show that the capacity of the cell using the bare $ZnSO_4$ decayed rapidly with increased voltage hysteresis compared with the Zn|$ZnSO_4$+Lys|$NH_4V_4O_{10}$ full

cell (Fig. 5e). Additionally, under a greater current density of 5 A/g, as shown in Fig. 5f, the Zn|$ZnSO_4$+Lys|$NH_4V_4O_{10}$ full cell exhibited stable cycling for 1000 cycles with a capacity retention of 72 % (170 mAh/g at the 1000^{th} cycle) and a consistent CE of around 99 %. By contrast, the capacity of the Zn|$ZnSO_4$|$NH_4V_4O_{10}$ full cell quickly decayed to 99 mAh/g after 260 cycles. The higher specific capacity of the full batteries might be ascribed to the side reaction-suppressing ability of the Lys additive, which can alleviate the capacity attenuation [68]. The SEM images (Fig. S13 in Supporting information) illustrate the uniform morphology of the Zn anode at 50^{th} cycle. Fig. S14 (Supporting information) shows the X-ray diffraction spectroscopy of the cycled zinc anode, the strengthened peak of the Zn(002) indicates that the Zn anode cycled in the $ZnSO_4$+Lys electrolyte exposed more (002) crystal planes, demonstrating the guidance of the Lys additive on Zn deposition [69]. Moreover, as shown in the magnified X-ray diffraction patterns, the peak of the by-products was reduced in the $ZnSO_4$+Lys electrolyte, indicating significant inhibition of side reactions by the Lys additive. In addition, as manganese-based materials are commonly applied in RAZIBs, full cells assembled with MnO_2 cathode (Fig. S15 in Supporting information) and Zn anode were fabricated to evaluate the universality of the Lys additive [70]. Fig. S14 shows that the Zn|$ZnSO_4$+Lys|MnO_2 full cell achieved an increased peak current and scanning area in the CV curve (Fig. S16 in Supporting information), which is consistent with the improved cycling performance of the full cell at 0.5 A/g (Fig. S17 in Supporting information).

In summary, the lysine (Lys) was introduced into the $ZnSO_4$ electrolyte to stablize the Zn anode by modifying the Zn anode–electrolyte interface. The Lys^+ cations could adsorb on the anode's surface and induce the 3D diffusion of Zn^{2+}, leading to the uniform deposition of Zn. Additionally, the incorporation of Lys into the bare 3 mol/L $ZnSO_4$ electrolyte caused a notable increase in the electrolyte's pH from 2.7 to 5.1, which favors the inhibition of HER and corrosion. Resultly, the cycling life of the Zn anode was significantly extended, demonstrating a remarkable lifetime of up to 4500 h at 1 mA/cm^2 (2400 h at 5 mA/cm^2 and 5 mAh/cm^2). The Zn||Cu cell utilizing the $ZnSO_4$+Lys electrolyte showcased highly reversible Zn plating/stripping behavior, accompanied by a high average Coulombic efficiency of 99 % maintained over 1200 cycles. Moreover, in the Zn||$NH_4V_4O_{10}$ full cell, stable operation was achieved for up to 1000 cycles at 5 A/g, while retaining 72 % of the initial capacity. This notable performance improvement underscores the effectiveness of the Lys additive in enhancing the operational efficiency of Zn anodes through interface modification. The findings from this study provide a new possibility for electrolyte additive engineering to improve highly stable zinc anode.

Declaration of competing interest

The authors declare that they have no known competing financial interests or personal relationships that could have appeared to influence the work reported in this paper.

CRediT authorship contribution statement

Guangbin Wang: Writing – original draft, Methodology, Formal analysis. **Binrui Xu:** Writing – review & editing, Methodology, Data curation. **Bo Zhao:** Software, Methodology. **Yifei Pei:** Investigation. **Haoming Li:** Visualization. **Wanhong Zhang:** Resources, Methodology, Data curation. **Yong Liu:** Writing – review & editing, Resources, Data curation, Conceptualization.

Acknowledgments

This work was supported by the National Key Research and Development Program of China (No. 2020YFB1713500), the Key Science and Technology Program of Henan Province (No. 232102241020), the Ph.D. Research Startup Foundation of Henan University of Science and Technology (No. 400613480015), the Natural Science Foundation of Henan Province (No. 242300420021), the Open Fund of State Key Laboratory of Advanced Refractories (No. SKLAR202210), the Student Research Training Plan of Henan University of Science and Technology (No. 2024054), and the Undergraduate Innovation and Entrepreneurship Training Program of Henan Province (No. S202310464012).

Supplementary materials

Supplementary material associated with this article can be found, in the online version, at doi:10.1016/j.cclet.2025.110859.

References

[1] L.E. Blanc, D. Kundu, L.F. Nazar, Joule 4 (2020) 771–799.
[2] Y. Geng, L. Pan, Z. Peng, et al., Energy Storage Mater. 51 (2022) 733–755.
[3] X. Xie, S. Wang, K. Kretschmer, et al., J. Colloid Interface Sci. 499 (2017) 17–32.
[4] H. Zhang, S. Li, L. Xu, et al., Adv. Energy Mater. 12 (2022) 2200665.
[5] Y. Liu, H. Wei, X. Zhai, et al., Mater. Design. 211 (2021) 110171.
[6] H. Qian, Y. Liu, H.X. Chen, et al., Energy Storage Mater. 58 (2023) 232–270.
[7] Z.X. Liu, S.H. Ha, Y. Liu, et al., J. Mater. Sci. Technol. 133 (2023) 165–182.
[8] Y.-M. Gao, Y. Liu, K.-J. Feng, et al., Rare Metals 43 (2024) 1–19.
[9] F. Wang, Y. Liu, H.J. Wei, et al., Rare Metals 40 (2021) 448–470.
[10] Y. Miao, Y. Zheng, F. Tao, et al., Chin. Chem. Lett. 34 (2023) 107121.
[11] D. Xie, F. Hu, X. Yu, et al., Chin. Chem. Lett. 31 (2020) 2268–2274.
[12] L. Wang, G. Fan, J. Liu, et al., Chin. Chem. Lett. 32 (2021) 1095–1100.
[13] E.Y. Hu, X.Q. Yang, Nat. Mater. 17 (2018) 480–481.
[14] J.F. Parker, C.N. Chervin, I.R. Pala, et al., Science 356 (2017) 415.
[15] G.Z. Fang, J. Zhou, A.Q. Pan, et al., ACS Energy Lett. 3 (2018) 2480–2501.
[16] S. Higashi, S.W. Lee, J.S. Lee, et al., Nat. Commun. 7 (2016) 11801.
[17] D.L. Zhu, Y.F. Zheng, Y. Xiong, et al., J. Alloys Compd. 918 (2022) 165486.
[18] Y. Liu, F. Tao, Y.B. Xing, et al., Molecules 28 (2023) 1742.
[19] L. Han, Y. Guo, F. Ning, et al., Adv. Mater. 36 (2023) 2308086.
[20] X. Yan, X. Huang, Y. Liu, et al., Chin. Chem. Lett. 35 (2024) 109426.
[21] B. Wu, Y. Mu, Z. Li, et al., Chin. Chem. Lett. 34 (2023) 107629.
[22] F. Tao, K.J. Feng, Y. Liu, et al., Nano Res. 16 (2022) 6789–6797.
[23] P.H. Zhai, X.L. Zhai, Z.H. Jia, et al., Nanotechnology 34 (2023) 085402.
[24] M. Sun, Z. Wang, J. Jiang, et al., Chin. Chem. Lett. 35 (2024) 109393.
[25] H. Tian, Z. Li, G. Feng, et al., Nat. Commun. 12 (2021) 237.
[26] J. Zheng, Q. Zhao, T. Tang, et al., Science 366 (2019) 645.
[27] Y.Z. Li, Y.B. Li, A.L. Pei, et al., Science 358 (2017) 506–510.
[28] F. Wang, O. Borodin, T. Gao, et al., Nat. Mater. 17 (2018) 543–549.
[29] X.H. Zeng, J.N. Hao, Z.J. Wang, et al., Energy Storage Mater. 20 (2019) 410–437.
[30] C. Deng, X. Xie, J. Han, et al., Adv. Funct. Mater. 31 (2021) 2103227.
[31] Y. Cui, Q. Zhao, X. Wu, et al., Angew. Chem. Int. Ed. 59 (2020) 16594–16601.
[32] H. He, H. Tong, X. Song, et al., J. Mater. Chem. A 8 (2020) 7836–7846.
[33] B. Li, X. Zhang, T. Wang, et al., Nano-Micro Lett. 14 (2022) 6.
[34] F. Tao, Y. Liu, X.Y. Ren, et al., J. Energy Chem. 66 (2022) 397–412.
[35] Y. Zhang, Z. Zeng, S. Yang, et al., Energy Storage Mater. 57 (2023) 557–567.
[36] X. Zhang, J. Li, K. Qi, et al., Adv. Mater. 34 (2022) 2205175.
[37] S. Yang, Y. Zhang, Y. Zhang, et al., Adv. Funct. Mater. 33 (2023) 2304280.
[38] X. Liu, Y. Fang, P. Liang, et al., Chin. Chem. Lett. 32 (2021) 2899–2903.
[39] D. Feng, F. Cao, L. Hou, et al., Small 17 (2021) 2103195.
[40] J. Zhou, Q. Li, X. Hu, et al., Chin. Chem. Lett. 35 (2024) 109143.
[41] Y. Liu, K. Feng, J. Han, et al., J. Mater. Sci. Technol. 211 (2025) 53–61.
[42] H. Zhang, R.T. Guo, S. Li, et al., Nano Energy 92 (2022) 106752.
[43] X. Wang, A.V. Kirianova, X. Xu, et al., Nanotechnology 33 (2022) 125401.
[44] F. Yang, J.A. Yuwono, J. Hao, et al., Adv. Mater. 34 (2022) 2206754.
[45] Z. Chen, H. Chen, Y. Che, et al., ACS Sustain. Chem. Eng. 9 (2021) 6855–6863.
[46] H. Lu, X. Zhang, M. Luo, et al., Adv. Funct. Mater. 31 (2021) 2103514.
[47] Z. Zhao, P. Li, Z. Zhang, et al., Chem. Eng. J. 454 (2023) 140435.
[48] D. Geng, Y. Tang, X. Han, et al., Int. J. Electrochem. Sci. 18 (2023) 100191.
[49] Z. Miao, Q. Liu, W. Wei, et al., Nano Energy 97 (2022) 107145.
[50] H.G. Akillioglu, M.N. Lund, Food Chem. 366 (2022) 130601.
[51] A. Yang, Q. Huang, Z. Wei, et al., CrystEngComm 24 (2022) 6400–6407.
[52] R. Krishna, E. Titus, R. Krishna, et al., J. Nanosci. Nanotechnol. 12 (2012) 6645–6651.
[53] H.T. Lu, X.L. Zhang, M.H. Luo, et al., Adv. Funct. Mater. 31 (2021) 2103514.
[54] X. Liang, X. Chen, Z. Zhai, et al., Chem. Eng. J. 480 (2024) 148040.
[55] M.M. Han, J.W. Huang, X.S. Xie, et al., Adv. Funct. Mater. 32 (2022) 2110957.
[56] N. Wang, X. Chen, H. Wan, et al., Adv. Funct. Mater. 33 (2023) 2300795.
[57] Z. Miao, Q. Liu, W. Wei, et al., Nano Energy 97 (2022) 107145.
[58] Q.W. Zhao, Y.Y. Wang, W. Liu, et al., Adv. Mater Interfaces 9 (2022) 2102254.
[59] W. Zhang, Y.H. Dai, R.W. Chen, et al., Angew. Chem. Int. Ed. 62 (2022) e202212695.
[60] R. Zhu, Z. Xiong, H. Yang, et al., Energy Storage Mater. 46 (2022) 223–232.
[61] J.Q. Zhou, L.F. Zhang, M.J. Peng, et al., Adv. Mater. 34 (2022) 2200131.
[62] R. Qin, Y. Wang, M. Zhang, et al., Nano Energy 80 (2021) 105478.
[63] H.B. Yan, S.M. Li, Y. Nan, et al., Adv. Energy Mater. 11 (2021) 2100186.

[64] S.S. Chi, Q.R. Wang, B. Han, et al., Nano Lett. 20 (2020) 2724–2732.
[65] Q. Zong, W. Du, C. Liu, et al., Nano-Micro Lett. 13 (2021) 116.
[66] B. Tang, J. Zhou, G. Fang, et al., J. Mater. Chem. A 7 (2019) 940–945.
[67] N. Hu, W. Lv, H. Tang, et al., J. Mater. Chem. A 11 (2023) 14921–14932.
[68] Y. Kim, Y. Park, M. Kim, et al., Nat. Commun. 13 (2022) 2371.
[69] T.T. Wei, Y.K. Ren, Y.F. Wang, et al., ACS Nano 17 (2023) 3765–3775.
[70] Y. Ma, M. Xu, R. Liu, et al., Energy Storage Mater. 48 (2022) 212–222.